Fission yeast cytokinesis requires a putative mechanosensitive channel Pkd2p

Qian Chen*, Zachary Morris and Brittni Morris

* Correspondence: qian.chen3@utoledo.edu

Department of Biological Sciences

University of Toledo

2801 West Bancroft ST

Toledo, OH, 43606

Running title: Yeast cytokinesis requires Pkd2p channel

Abbreviations: Transient receptor potential (TRP), Autosomal Polycystic Kidney Disease (ADPKD), Septation initiation network (SIN), Methyl benzimidazol-2-carbamate (MBC), Latrunculin A (LatA), Mitogen-associated protein kinase (MAPK)

Abstract:

Mechanical force applied by the actomyosin contractile ring plays an essential role in separating the daughter cells during cytokinesis, the last stage of cell division. However, it remains largely unknown how the dividing cell senses and adapts to this force. We discovered that fission yeast recruit Pkd2p, a putative force-sensing ion channel, to the cell division site in cytokinesis. Pkd2p is an essential protein and the homologue of a human mechanosensitive channel polycystin-2 that is associated with Autosomal Polycystic Kidney Disease (ADPKD). Depletion of Pkd2p resulted in 50% faster constriction of the contractile ring, compared to the wild type cells. This led to strong defects in the septum assembly and the abscission of daughter cells. The *pkd2* mutant also showed strong positive genetic interaction with the SIN signaling pathway that regulates fission yeast septation. Many *pkd2* depleted cells deflated temporarily under mechanical stress, losing ~30% of their volume. They activated the MAPK kinase Sty1p-mediated stress response pathway and suspended many essential cellular processes including mitosis and cytokinesis, leading up to their recovery in 30 min. We concluded that Pkd2p attenuates both the contractile ring constriction and the SIN pathway in cytokinesis, potentially as a putative force-sensing channel.

Highlight summary for TOC:

In studying how cells sense the mechanical force in cytokinesis, we discovered that fission yeast Pkd2p, a putative mechanosensitive channel, localizes to the cleavage furrow. It attenuates the contractile ring constriction and the septation signaling pathway. Its depletion resulted in cytokinesis defects, deflated cells and stress responses.

Introduction:

Force plays a central role in separating daughter cells during cytokinesis, the last stage of cell division (for review see (Pollard, 2010; Srivastava et al., 2016)). Since Ray Rappaport first measured the force required for abscission of daughter cells in cytokinesis (Rappaport, 1967), many follow-up studies have demonstrated the contractile ring applies the mechanical force through a myosin II-driven process that slides the actin filaments against each other in the ring (De Lozanne and Spudich, 1987; Sanger and Sanger, 1980; Straight et al., 2003). However, few studies have examined how the dividing cell could sense and adapt to this mechanical force required for cytokinesis, except for a few that were focused on the mechanosensitivity of myosin II (Effler et al., 2006).

Cytokinesis in fission yeast *Schizosacchromyces pombe* is largely conserved in animal cells (Pollard and Wu, 2010). Genetic studies have identified in it a large number of cytokinesis genes, most of which have homologues in human (Balasubramanian et al., 1998; Johnson et al., 2012). The molecular numbers of these proteins have also been measured through quantitative fluorescence microscopy (Courtemanche et al., 2016; Wu and Pollard, 2005). Similar to animal cells, the force generated by the contractile ring plays an important role in fission yeast cytokinesis (Stachowiak et al., 2014). The septum, newly synthesized cell wall at the cell division site, provides additional compression force required for cytokinesis (Proctor et al., 2012). Nevertheless, the mechanism of force-sensing in fission yeast cytokinesis remains largely unexplored.

One of the most important force-sensing mechanisms is through the unique activities of mechanosensitive channels (Kung, 2005). These force-gated channels respond to mechanical cues to regulate homeostasis of intracellular ion concentration, activating the downstream

signaling pathways. They were first identified in bacteria as channels that sense osmotic pressure (Martinac et al., 1987). Since then, many more such channels have been found in multicellular organisms for their role in sensing touch, vibration and flow (Mochizuki et al., 1996; Nauli et al., 2003; Walker et al., 2000). Many of them belong to the evolutionally conserved transient receptor potential (TRP) family of ion channels (Montell and Rubin, 1989) (for review see (Wu et al., 2010)), which have also been found in yeast (Palmer et al., 2005; Palmer et al., 2001).

In this study, we examined whether any of fission yeast TRP channels plays a role in cytokinesis. We discovered that one of them Pkd2p is potentially a new regulator of cytokinesis. Pkd2p belongs to polycystin-2 subfamily of mechanosensitive channels that are conserved in most eukaryotes. Its founding member is human polycystin-2, a calcium-permeable non-selective cation channel (Gonzalez-Perrett et al., 2001; Grieben et al., 2017; Shen et al., 2016; Wilkes et al., 2017). Loss of function mutations in human polycystin-2 are associated with a common hereditary renal disorder Autosomal Polycystic Kidney Disease (ADPKD). Polycystin-2 plays important roles in many other developmental processes as well including cardiac development and left-right orientation (Pennekamp et al., 2002; Wu et al., 2000) through its mechanosensing ability (Nauli et al., 2003). Here we set out to determine the little studied role of Pkd2p in cytokinesis.

Results:

A putative fission yeast TRP channel Pkd2p localizes to the cell division site

We examined the cell-cycle dependent localization of all three putative TRP channels in fission yeast. We tagged each one of them, Trp663p, Trp1322p and Pkd2p (Aydar and Palmer, 2009; Ma et al., 2011; Palmer et al., 2005) with at its C-terminus with mEGFP. Live fluorescence microscopy showed that only Pkd2p-mEGFP was recruited to the cell division site during

cytokinesis (Fig. 1A and 1B, Movie S1). Neither morphology nor viability of *pkd2::pkd2-mEGFP* cells showed any difference from those of the wild type cells (Fig. 1B). Because *pkd2* is an essential gene (Palmer et al., 2005) (Fig. 2B), we concluded that Pkd2-mEGFP is a functional replacement of the endogenous protein that localizes to the cleavage furrow in cytokinesis.

The localization of Pkd2p is cell-cycle dependent. In interphase, Pkd2p-mEGFP localized preferentially to the two poles in addition to the intracellular vesicles (Fig. 1A and Movie S1), consistent with what had been found through immunofluorescence microscopy (Palmer et al., 2005). Quantitative fluorescence microscopy showed that Pkd2p-GFP molecules started to accumulate at the cleavage furrow when the contractile ring started to constrict (Fig. 1B and 1C). A three-dimension reconstruction of the cleavage furrow showed that Pkd2p-GFP localized in a donut-shaped disk that constricted concomitantly with the contractile ring (Fig. 1C). The molecular number of Pkd2p-GFP molecules at the furrow reached a peak of ~1,200 when the contractile ring constricted completely (Fig. 1D), before their dispersal to the poles of two daughter cells (Movie S1).

The localization of Pkd2p at the cleavage furrow depends on the actin cytoskeleton but not on the microtubules. Depolymerization of actin filaments with latrunculin A completely displaced Pkd2p-mGFP from the furrow (Fig. 1E). In the absence of the contractile ring in these LatA treated cells, Pkd2p localized to discreet puncta on the plasma membrane adjacent to the clumps marked by myosin II (Fig. S1A). On the other hand, depolymerization of the microtubules by MBC had no effect on the localization of Pkd2p in cytokinesis (Fig. S1B). We concluded that Pkd2p, a putative ion channel localized at the cleavage furrow, is likely a novel component of the fission yeast cytokinetic machinery.

Pkd2 is an essential gene required for both cell growth and cell division

Pkd2 is the homologue of human polycystin-2, a mechanosensitive ion channel (Palmer et al., 2005). Fission yeast Pkd2p possesses an MD-2-related lipid-recognition (ML-2) domain (Inohara and Nunez, 2002), a central TRP like domain and a C-terminal coiled-coil domain (Fig. 2A). Our analysis also showed that the first 23 amino acids of Pkd2p, the predicted signal peptide, will be cleaved before the protein reaches its destination.

We first confirmed that *pkd2* is an essential gene (Fig. 2B). Tetrad dissection of *pkd2*$^{+}$*/pkd2Δ* showed that *pkd2Δ* cells were not viable, agreeing with a previous study that used random spore analysis (Palmer et al., 2005). Stabilizing cell wall through the addition of 1.2M sorbitol in the media did not rescue the viability of *pkd2Δ* cells (Fig. 2B), suggesting that the activity of Pkd2 is required for more than maintaining the cell wall integrity as proposed previously (Aydar and Palmer, 2009).

To determine the function of Pkd2p in cytokinesis, we made three *pkd2* mutants by replacing its endogenous promoter with one of three fission yeast inducible promoters, *P3nmt1* (strong), *P41nmt1* (intermediate) or *P81nmt1* (weak) respectively (Basi et al., 1993; Maundrell, 1990). We examined both viability and morphology of three mutants under either suppressing or inducing condition (Fig. 2C). As we expected, *pkd2::P41nmt1-pkd2* cells appeared indistinguishable from the wild type cells under either conditions. Surprisingly, over-expression of Pkd2p in *pkd2::P3nmt1-pkd2* cells under the inducing condition had no apparent effect on either their viability or morphology (Fig. 2C). In comparison, depletion of Pkd2p under the suppressing condition, in *pkd2::P81nmt1-pkd2* which we would refer to as *pkd2-81KD* from this point on, induced a wide range of defects.

Depletion of Pkd2p resulted in strong defects in both cell morphology and cell growth. These *pkd2* mutant cells are 10% wider and more irregular shaped than the wild type cells,

defects that were largely rescued by restoring the expression of Pkd2p (Fig. 2C). They were also hypersensitive to high concentration of salts (Fig. 2D). We found that the mutant was most sensitive to $CaCl_2$ but it was also sensitive to KCl and $MgCl_2$ (Fig. 2D).

We found that depletion of Pkd2p resulted in a particularly strong defect in the separation of daughter cells, the last stage of cytokinesis. The fraction of *pkd2-81KD* cells with septum was about three times higher than that of the wild type cells (Fig. 3A and 3B). We compared the process of daughter cell separation in the wild type cells to that in the *pkd2* mutant cells with time-lapse bright field microscopy that could readily identify the septum (Fig. 3C). After the septum assembled at the cell division site of a wild type cell, it gradually thinned out in 59 ± 8 mins (average ± standard deviation), coinciding with the abscission of daughter cells (Fig. 3D). In comparison, the septum of the *pkd2* mutant cells often persisted for a very long time (Fig. 3C). During this period, the likely defective septum thickened continuously and swing from side to side, appearing to be under pressure (Fig. 3C). Overall, it took almost twice as long, 111 ± 21 min for the *pkd2* mutant cells to assemble the septum and separate the daughter cells. Many mutant cells failed to abscise at all in more than 2 hrs (Fig. 3D and Movie S2). We concluded that Pkd2p is essential for the abscission of daughter cells in cytokinesis.

Pkd2p modulates the constriction of the contractile ring in cytokinesis

To understand the molecular role of Pkd2p in cytokinesis, we first analyzed the assembly, the maturation and the constriction of the contractile ring in *pkd2-81KD* cells. The abscission in fission yeast cytokinesis depends on the septum, whose placement and expansion are tightly coupled to the contractile ring. The contractile ring is assembled ~10 min after the separation of the spindle pole bodies (SPB) (Wu et al., 2003), a process that requires the activity of Myo2p, Cdc12p and cofilin (Balasubramanian et al., 1998; Chang et al., 1997; Chen and Pollard, 2011).

During the maturation, the contractile ring continues to add actin filaments (Courtemanche et al., 2016) and recruits many other cytokinesis proteins (Wu et al., 2003). This is followed by the Myo2p-driven constriction of the contractile ring which lasts ~30 min (Laplante et al., 2015; Mishra et al., 2013). To facilitate the quantitative analysis, we used the separation of SPBs, marked by Sad1p-mEGFP, as the reference point (time zero, (Wu et al., 2003)) and myosin light chain, Rlc1p, tagged with tdTomato, as a marker for the contractile ring (Fig. 4A).

We found no significant defect in the contractile ring assembly and maturation in *pkd2-81KD* cells (Fig. 4A and 4B, Movie S3 and S4). The assembly of the contractile ring was slightly slower in the mutant cells, compared to that of the wild type cells while the maturation remained largely unchanged (Fig. 4A). Combined, these two processes only took slighter longer time in the mutant than they did in the wild type cells (29 ± 4 vs. 25 ± 4 mins, average ± standard deviation, $P < 0.001$) (Fig. 4B).

In contrast, we found that the contractile ring constricted much faster in the *pkd2* mutants, than it did in the wild type cells. The rate of the ring constriction in the wild type cells was 0.30 ± 0.04 μm/min (Fig. 4C-4E), in line with previously published results (Chen and Pollard, 2011; Laplante et al., 2015). Depletion of Pkd2p increased the constriction rate by more than 50% to 0.47 ± 0.07 μm/min (Fig. 4C-4E, $P < 0.0001$). Conversely, the duration of the ring constriction was reduced significantly in these cells (Fig. 4C). We concluded that a key function of Pkd2p in cytokinesis is to attenuate the contractile ring constriction, but how this is linked to the defect in the separation of daughter cells in *pkd2-81KD* remained unexplained.

To answer this question, we examined the septum assembly during the abscission in these *pkd2* mutant cells. Fission yeast cytokinesis requires the septum which expands in sync with the contractile ring constriction. Its assembly at the cell division site requires at least four glucan

synthases, including Bgs1p for the primary septum and Bgs4p for the secondary septum respectively (Cortes et al., 2012; Liu et al., 1999; Munoz et al., 2013). Both GFP-Bgs1p and GFP-Bgs1p localized to the cell division site in the mutant cells, similar to how they localized in the wild type cells (Fig. 5A). However, we found with quantitative fluorescence microscopy that the number of GFP-Bgs1p molecules decreased by ~20% but the number of GFP-Bgs4p molecules increased by ~50% at the cell division site of the *pkd2* mutant, compared to the wild type cells (Fig. 5B-5E). The decrease of GFP-Bgs1p molecules in the septum of the mutant cells was expected, given these cells had less time to recruit them to the cell division site because of the faster ring constriction compared to the wild type cells (Fig. 5B ad 5D). The increase of GFP-Bgs4p in the septum was surprising, which may be a compensating mechanism by the cells. As a result, the ratio of the peak number of GFP-Bgs4p to GFP-Bgs1p molecules (Fig. 5D and 5E), two glucan synthases required for the synthesis of the primary and secondary septum respectively, increased by ~80% in the *pkd2* mutant cells (Fig. 5F). This potentially altered the structure of the septum in these *pkd2* mutant cells significantly. We concluded that Pkd2p, through attenuating the speed of the contractile ring constriction, regulates the septum assembly in cytokinesis.

Pkd2p modulates the signaling pathway of septation in cytokinesis

In fission yeast cytokinesis, the abscission of daughter cells also requires the septation initiation network (SIN), a fission yeast Hppo-like kinase cascade (Balasubramanian et al., 1998; Johnson et al., 2012; Simanis, 2015). To understand the role of Pkd2p in the abscission, we determined whether the *pkd2* mutant has any genetic interaction with temperature mutants of the SIN pathway.

We identified strong genetic interactions between *pkd2* and the SIN pathway. *pkd2-81KD* had positive genetic interaction with two mutants of the SIN pathway, *sid2-250* and *mob1-R4,* the temperature sensitive mutants of Sid2p kinase and its activator Mob1p respectively (Balasubramanian et al., 1998; Hou et al., 2000) (Fig. 6A). Both genes sit at the bottom of the SIN pathway hierarchy and the proteins are only SIN pathway components localized to the cleavage furrow during cytokinesis (Sparks et al., 1999; Wu et al., 2003). Consistent with the genetic interactions, we found that the depletion of Pkd2p strongly rescued both lysis and septation defects of the two SIN mutants at either semi-restrictive (33°C) or restrictive temperature (36°C) (Fig. 6B and 6C). We conclude that Pkd2p also attenuates activities of the SIN pathway in cytokinesis.

Pkd2 mutant cells are under acute stress

Besides their cytokinesis defects, many *pkd2-81KD* mutant cells oscillated between "deflated" and "inflated" states. Among the *pkd2-81KD* mutant cells that we followed for up to 3 hrs, 22% of them shrank temporarily, losing both length and width during this "deflated" state (Fig. 7A and Movie S5). These cells lost close to 30% of their volume within a few minutes. Surprisingly, most of them (74%, n = 103) recovered their volume within 30 min, back to the "inflated" state. The mutant cells behaved similarly to the wild type cells did under osmotic stress, even though the mutant cells were cultured in an isotonic environment. We proceeded to examine whether these *pkd2* depleted cells displayed hallmarks of cellular stress in the "deflated" state.

First, we determined whether the MAPK stress response pathway is activated in these pkd2 mutant cells. In fission yeast, stress activates the mitogen-associated protein kinase (MAPK) Sty1p-mediated signaling cascade (Degols et al., 1996; Millar et al., 1995; Shiozaki and Russell, 1995). In response to the stress such as 1 M KCl, Sty1p, is shuttled into nucleus to

activate various transcription factors to ensure adaptation (Fig. S2A), as reported (Gaits et al., 1998). Not surprisingly, the MAPK Sty1p mediated stress response pathway was hyper-activated in *pkd2-81KD* cells. Although the total number of Sty1p-mEGFP molecules remained unchanged, the fraction of the mutant cells with elevated nuclear localization of Sty1p-GFP increased significantly compared to that of the wild type cells (Fig. 7B). Sty1p-mEGFP started to shuttle into the nucleus when the *pkd2* mutant cells started to deflate (Fig. 7C-7D and Movie S6). The accumulation of Sty1p-GFP in the nucleus continue for more than ten minutes, reaching a three-fold increase compared to the pre-deflated state (Fig. 7D). As the mutant cells slowly recovered their original volume, the number of Sty1p-GFP molecules in the nucleus of the mutant cells gradually decreased to that in the pre-deflated cells (Fig. 7C). The whole process took around 40 mins (Movie S6).

Similar to other stressed cells, the *pkd2* mutant cells suspended most cellular processes including mitosis, cytokinesis and endocytosis when they entered the "deflated" state. In mitosis, we found that mitotic progression paused in these mutant cells (Fig. 8A), another sign of cells under stress (Shiozaki and Russell, 1995). In cytokinesis, these "deflated" mutant cells stopped the contractile ring constriction temporarily in cytokinesis (Fig. 7B and Movie S7). This pause usually lasted about 10-20 mins, during which the contractile rings appeared buckled under mechanical force (Fig. 7B). In endocytosis, the patch of deflated *pkd2-81KD* cells underwent turnover much more slowly (Fig. S2B), compared to the actin patch of the wild type cells with a lifetime of ~20 seconds (Chen and Pollard, 2013; Sirotkin et al., 2010). Lastly, we found that turnover of the interphase microtubules slowed down dramatically in the deflated mutant cells (Movie S8). We concluded that depletion of Pkd2p led to the mutant cells under strong mechanical stress.

In summary, we discovered Pkd2p as a novel regulator of cytokinesis in fission yeast. Pkd2p, a putative mechanosensitive channel, localizes to the cleavage furrow. It modulates both the constriction of the contractile ring and the signaling pathway of septation in cytokinesis. In its absence, the mutant cells face severe mechanical stress that activates the MAPK pathway and arrests the turnover of cellular cytoskeleton. We proposed that Pkd2p, activated by the force in cytokinesis, functions as a force-sensitive channel in a negative feedback loop to attenuate ingression of the cleavage furrow and prevent mechanical damage to the dividing cell (Fig. 9).

Discussion:

Despite of the importance of mechanical force in cytokinesis, the molecular mechanism of force-sensing in cell division remains largely unknown. We discovered in this study that the fission yeast Pkd2p, a putative mechanosensitive channel, may play an essential role in force-sensing in cytokinesis.

Pkd2p likely functions as a "brake" in cytokinesis

We propose that Pkd2p functions as a "brake" in cytokinesis to attenuate the force that drives the constriction of the contractile ring. It is supported by our observation the in the *pkd2* mutant cells, the contractile ring constricts significantly more quickly than normal. It is also consistent with our finding that the primary septum, marked by GFP-Bgs1p, expanded more quickly in the *pkd2* mutant, compared to the wild type cells.

We expect two potential defects, as a result of the accelerated ring constriction when the "brake" is compromised. First, it may lead to a mechanical damage to the plasma membrane at the cell division site, because of the faster than normal ingression of the cleavage furrow. Secondly, it may prevent the assembly of a fully functional primary septum whose expansion is coupled to the ring constriction. Either scenario may explain frequent failure in the abscission of

daughter cells and the severe stress in the Pkd2p depleted cells. We found that ratio of two glucan synthases, Bgs1p and Bgs4p, in the septum is substantially changed in the septum of the pkd2 mutant cells. This suggested that a defect in the septum assembly may partially explain the abscission defect of the *pkd2* mutant.

The ion channel activities of Pkd2p in cytokinesis

We propose that Pkd2p likely functions as an ion channel at the cleavage furrow in cytokinesis. Pkd2p belongs to the polycystin-2 family of nonselective cation channels (Gonzalez-Perrett et al., 2002; Liu et al., 2018; Shen et al., 2016). Two earlier studies showed that fission yeast Pkd2p likely function as an ion channel as well (Aydar and Palmer, 2009; Palmer et al., 2005). Our data also supported this hypothesis in showing that the *pkd2* depleted cells are hypersensitive to calcium, potassium and sodium. Lastly, two of the four budding yeast *pkd2* orthologues, Flc1p and Flc2p, regulate the intracellular calcium homeostasis (Protchenko et al., 2006; Rigamonti et al., 2015; Vazquez et al., 2016).

Fission yeast Pkd2p is likely a constitutively inactive channel. This is supported by our data showing that over-expression of Pkd2p did not lead to any defects in cytokinesis, cell morphology or cell growth. Human polycystin-2, a homologue of Pkd2p, is a cation channel activated by mechanical cues (Nauli et al., 2003; Shen et al., 2016). We propose that both the contractile ring and the septum might generate the mechanical force required to activate Pkd2p in fission yeast cytokinesis.

Fission yeast Pkd2p channel may regulate the local calcium concentration at the cell division site during cytokinesis. In many organisms, calcium concentration at the cleavage furrow spikes during cytokinesis (Fluck et al., 1991; Miller et al., 1993) but the mechanism and its importance remains unclear (Noguchi and Mabuchi, 2002). It remains unknown whether there

is a similar increase of calcium concentration at the cell division site in fission yeast. It is worth noting that the calcium dependent phosphatase calcineurin does localize to the cleavage furrow (McDonald et al., 2017).

Localization of Pkd2p channel during cell division

Our study demonstrated surprisingly that a putative ion channel localizes to the cleavage furrow during fission yeast cytokinesis. Although it has been shown that Pkd2p localizes to both the intracellular organelles and the plasma membrane in interphase (Aydar and Palmer, 2009; Palmer et al., 2005), its localization in cell division has never been examined. We only found in a fission yeast proteomics study showing that Pkd2-YFP, expressed from a plasmid, localize to the cell division site (Riken *S. pombe* Postgenome Database). To our knowledge, few studies have characterized the localization of the other Pkd2p homologues in cell division either. This is likely due to their well-documented localization in cilia (Barr et al., 2001; Barr and Sternberg, 1999; Gao et al., 2003; Watnick et al., 2003) which disassemble in mitosis. Among few studies that examined the localization of ion channels in cell division, one showed that TRPC1, a TRP channel like Pkd2p, localizes at the cleavage furrow of dividing zebrafish embryos (Chan et al., 2016; Chan et al., 2015). More studies are required to explore the role of ion channels, particularly those calcium permeable channels, in cell division.

Pkd2 and the underlying molecular mechanism of ADPKD

Although Pkd2p plays an essential role in many biological processes, the underlying molecular mechanism remains obscure. Pkd2p homologues are required for male fertility in both fruit fly and worm (Barr and Sternberg, 1999; Gao et al., 2003; Watnick et al., 2003). On the other hand, the human homologue polycystin-2 plays an essential role in the kidney epithelial cells (Wu et al., 1998). Loss of function mutations in polycystin-2 accounts for 15% of Autosomal Dominant

Polycystic Kidney Disease (ADPKD) cases (Mochizuki et al., 1996). Mutations in polycystin-1, a binding partner of polycystin-2 (Qian et al., 1997; Tsiokas et al., 1997), accounts for the other 85% (Hughes et al., 1995). The hallmark of ADPKD is development of liquid-filled cyst in the patient's kidney. The symptom will get progressively worse until daily dialysis is needed for the end-stage patients. There are some similarities between the defects found in the kidney epithelial cells of ADPKD patients and the yeast *pkd2* mutant despite these two homologues are separated by millions of years of evolution. Both mutant cells increase their sizes significantly and are under chronical stress. We expect that the study of the molecular function of Pkd2p will provide us novel insights into how mutations in human polycystin-2 contribute to the prognosis of ADPKD. (949 words)

Materials and Methods:

Yeast genetics

Yeast cells were cultured according to the standard methods. We constructed *trp663::trp663-GFP*, *trp1322::trp1322-GFP, pkd2::pkd2-GFP* and *pkd2::pkd2(1-576)-GFP* by integrating the sequence of mEGFP at the endogenous locus through PCR based homologous recombination. (Bahler et al., 1998). To examine the viability of *pkd2Δ*, we constructed $pkd2^{+}/pkd2\Delta$ diploid strain by deleting the endogenous ORF through homologous recombination in a wild type diploid strain. The $pkd2^{+}/pkd2\Delta$ cells were sporulated on SPA5s plates and dissected into more than 20 tetrads. The *pkd2::kanMX6* spores were selected with 100 µg/ml G418. To replace the endogenous *pkd2* promoter, we integrated the inducible nmt1 promoters to precede the start codon (ATG) of the *pkd2* ORF at its endogenous locus. The resulting yeast strains were confirmed by PCR and the Sanger sequencing method. Tetrad dissection was carried out with a SporePlay+ dissection microscope (Singer, England). To image the temperature-sensitive

mutants, they were inoculated at the permissive temperature for 2 days before being shifted to the restrictive temperature for 4 hrs before experiments.

Fluorescence microscopy

For microscopy, we grew yeast cells in liquid YE5s medium for two days before harvesting the exponentially growing culture at a density between $5.0*10^6$ cells/ml to $1.0*10^7$ cells/ml by centrifugation at 4,000 rpm for 1 min. The cells were re-suspended in YE5s before being applyin to a 25% gelatin + YE5s pad, sealed under the coverslip with VALEP (a mix of equal amount of Vaselin, lanolin and paraffin). Live microscopy was carried out on an Olympus IX71 microscope equipped with a 100x (NA = 1.41) objective lens, a confocal spinning disk unit (CSU-X1, Yokogawa, Japan), a motorized XY stage and a Piezo Z Top plate (ASI, USA). The images were acquired with an Ixon-897 EMCCD camera controlled by iQ3.0 (Andor, Ireland). Two lines, 488 nm and 561 nm, of solid state laser were used in the confocal fluorescence microscopy, at power of less than 5 mW. Unless specified, we acquired 15 slices at a step-size of 0.5 μm for Z-series. Live microscopy was carried out in a room where the temperature was maintained at around 23°C. To minimize variations, we usually imaged the wild type and the mutant cells on the same day. For visualizing cell wall, we stained the yeast cells with 10 μg/ml of calcofluor (Sigma) and used an Olympus IX81 microscope equipped with a CCD camera and a mercury lamp for the epifluorescence microscopy.

Image processing

We used Image J (NIH) to process all the images, with either freely available or customized macros/plug-ins. For quantitative analysis, the fluorescence micrographs were corrected for drifting by StackReg plug-in (Thevenaz et al., 1998) and for photo-bleaching by EMBLTools plug-in (Rietdorf, EMBL Heidelberg). The sums of all Z-slices were used for quantification. The

contractile ring localization of Pkd2p-GFP was analyzed by quantifying the fluorescence in a 3.6 μm by 0.8 μm (36 by 8 pixels) rectangle centering on the cell division site, corrected with background subtraction. The molecular numbers of GFP-Bgs1p and GFP-Bgs4p were quantified similarly. The ring constriction rate is calculated as π*D/T. D represents the diameter of the contractile ring, measured before it starts to constrict. T presents the duration of the ring constriction. It is measured by examining a fluorescence micrograph constructed from the time-lapse videos to determine both the start and the end of the constriction. The nuclear localization of Sty1p-GFP was analyzed by quantifying its fluorescence intensities in the nucleus. To simplify the analysis, we assume the nucleus as a circle of 2μm diameter determined by the nucleus localization of Sty1p-GFP. The quantification was corrected with background subtraction by measuring the fluorescence intensities of Sty1p-GFP in the cytoplasm around the nucleus. To measure total area of the cells expressing Sty1p-GFP, we segmented the cells based upon the cytoplasmic fluorescence of Styp1-GFP. Our confocal microscope was calibrated using a previously published method (Wu and Pollard, 2005). Briefly, we imaged seven GFP tagged fission yeast strains and made a calibration curve of fluorescence vs. molecular number ($R^2 >$ 0.95). The slope of the calibration curve was used to convert the value of the fluorescence intensities to the number of molecules. The figures were made with Canvas X (ACDsee systems, Canada). The domain structure of Pkd2p is based on the prediction by Pfam and NCBI.

Acknowledgement:

Q.C. designed the study. Q.C., Z.M. and B.M., carried out the experiment. Q.C. wrote the manuscript. This work is supported by the University of Toledo Start-up Fund and deArce-Koch Memorial Endowment Fund to Q.C.. We would like to thank Juan Carlos Ribas (University of Salamanca, Spain), Jianqiu Wu (Ohio State University) and Daniel McCollum (University of

Massachusetts Medical School) for generously sharing yeast strains with us. The authors would like to thank their colleagues at the Department of Biological Sciences, Song-Tao Liu, Richard Komuniecki and Jianyang Du, for providing critical insights in the preparation of this manuscript.

Figure legends:

Fig. 1 Pkd2 localizes to the site of cell division during cytokinesis. (A) Fluorescence micrographs of fission yeast cells expressing Trp663p-GFP and Trp1322p-GFP respectively. (B-C) Pkd2p-GFP (green) and Rlc1p-tdTomoato (red). Maxim intensity projections are shown. (B) The merged image is shown on the right. (C) The merged time-lapse fluorescence micrographs of the cleavage furrow in a dividing cell. Head-on views, reconstructed from the Z-series, are shown. Numbers represent minutes. (D) Average time course of the number of Pkd2p-mEGFP molecules at the cell division site. Error bars represent standard deviations. Time zero coincides with the starts of the contractile ring constriction. (E) Fluorescence micrographs of the cells expressing Pkd2p-mEGFP, treated with either control (DMSO, left) or 10 μM latrunculin A (LatA, right) Depolymerization of actin filaments with LatA displaced Pkd2p-GFP from the contractile ring (red arrow heads) to the cortex clumps at the cell-division site (red brackets). Bars represent 5 μm.

Figure 2 Pkd2p is an essential gene and its depletion led to shrinkage during cell division. **(**A) The predicted domain structure by Pfam (top) of fission yeast Pkd2p. ML-like domain: MD-2-related lipid recognition domain. CC: coiled-coil domain. (B) Dissected tetrads from sporulated *pkd2*$^{+}$*/pkd2Δ* cells on either YE5s (top) or YE5s supplemented with 1.2 M sorbitol (bottom) plates. Red circles: where the *pkd2Δ* colonies shall have been. (C) Bright field micrographs of *pkd2::P81nmt1-pkd2* (left), *pkd2::P41nmt1-pkd2* and *pkd2::P3nmt1-pkd2*

(right) cells incubated in either YE5s (suppressing) or EMM5s (inducing) medium. Depletion of Pkd2p led to strong morphological defects but the over-expression did not. Arrow head points to multi-septated cells and arrow points to "deflated" cell. Bar represent 5 μm. (D) Ten-fold dilution series of the wild type and *pkd2::P81nmt1-pkd2* cells grown on YE5s plates supplemented with 0.2M $MgCl_2$, 1M KCl or 50mM $CaCl_2$. The plates were incubated at 30°C for 2 days.

Figure 3. Pkd2p is required for abscission of daughter cells in fission yeast cytokinesis. (A) Fluorescence micrographs of calcofluor stained wild type (*pkd2*$^+$) and *pkd2-81KD* cells. Arrow heads: bended septum in the *pkd2* mutants. (B) A bar graph showing the septation index of the wild type (gray) and *pkd2-81KD* (red) mutants (n > 500). Error bars show standard deviations. (C) The *pkd2* mutant failed to abscise. Top: a cartoon representation of the typical septation process in either the wild type or *pkd2-18KD* cells. Bottom: time lapse micrographs of a wild type (top) and a *pkd2-81KD* (bottom) imaged with bright field microscopy. After appearance of the septum (green) in the wild type cell, it thickened gradually before the abscission (red asterisk, 44 mins). In comparison, the septum in *pkd2-81KD* cells appeared bend under pressure and thickened continuously for an extended period of time (> 100 mins). Number represent time in minutes. (D) A histogram showing the duration of septation in either the wild type or *pkd2-81KD* mutants. Bars represent 5 μm.

Figure 4: The constriction of the contractile ring accelerated in cytokinesis of the *pkd2* mutant. (A) Merged time lapse fluorescence micrographs of either a wild type (top, *pkd2*$^+$) or a *pkd2-81KD* cell expressing both a contractile ring marker Rlc1p-Tdmato (Red) and a spindle pole body (SPB) marker Sad1p-GFP (Green). Time zero: when two SPBs (arrow heads) separated. Asterisk indicates when the contractile ring is assembled. Number represents time in

minutes. (B) Box plots of duration of the contractile ring assembly plus maturation in either the wild type (grey) or *pkd2-81KD* cells (red). The horizontal line represents the average. It take slightly longer time for the ring to assemble and mature the contractile in the mutant, compared to the wild type cells ($P < 0.001$). (C) Time lapse fluorescence micrographs of the ring constriction in either a wild type (top) or a *pkd2-81KD* cell (bottom) expressing Rlc1p-tdTomato. Only the median plane of a dividing cell is shown. Number represents time in minutes. (D) Fluorescence kymographs of the ring constriction in either a wild type (top) or a *pkd2-81KD* cell (bottom) expressing Rlc1p-tdTomato. (E) Box plots of rates of the contractile ring constriction in either the wild type (grey) or *pkd2-81KD* cells (red). The horizontal line represents the average. Bars represent 5 μm.

Figure 5. Pkd2p is required for proper assembly of the septum. (A) Fluorescence micrographs of the wild type (*pkd2*$^{+}$, top) and *pkd2-81KD* cells expressing either GFP-Bgs1p or GFP-Bgs4p. (B-C) Time lapse fluorescence micrographs of either a wild type (top) or a *pkd2-81KD* (bottom) cell expressing either GFP-Bgs1p (B) or GFP-Bgs4p (C). Interval between each frame is 2 min. Only the cell division site is shown. Asterisk represents completion of the primary septum expansion. (D) Average time course of the number of either GFP-Bgs1p molecules at the cell division site of either the wild type (blue line, n = 5) or *pkd2-81KD* (red line, n = 6) cells in cytokinesis. (E) Average time course of the number of either GFP-Bgs4p molecules at the cell division site of either the wild type (blue line, n = 6) or *pkd2-81KD* (red line, n = 6) cells in cytokinesis. Error bars represent standard deviations. (F) A bar graph showing the ratio of the molecular number of GFP-Bgs4p to that of GFP-Bgs4p when they reached the peak (time zero) at the cell division site in cytokinesis. Bars represent 5 μm.

Figure 6. Pkd2p modulates activities of the SIN pathway in cytokinesis. (A) Ten-fold dilution series of the wild type (*WT*) and the indicated mutant cells grown on YE5s plates. The plates were incubated at the indicated temperature for 2 days. We found strong positive genetic interactions between *pkd2-81KD* and either *mob1-R4* or *sid2-250*. (B-C) Bright field micrographs of *mob1-R4* (top left), *sid2-250* (top right), *pkd2-81KD mob1-R4* (bottom left) and *pkd-81KD sid2-250* (bottom right) cells inoculated at either 33°C (B) or 36°C (C) for 4 hrs. The depletion of *pkd2* largely rescued both the lysis (arrow head) and the septation defects (arrow) of the two SIN mutants at either semi-restrictive or restrictive temperature.

Figure 7. The Pkd2p depleted cells are under chronicle stress. (A) Time lapse micrographs of *pkd2-81KD* cells in YE5s medium, acquired with bright-field microscopy. Cell 1: a lysed cell. Cell 2 and 3: two cells that deflated before recovering. Numbers represents times in minutes. (B) Fluorescence micrographs of the wild type (*pkd2*$^{+}$, left) and *pkd2-81KD* mutant cells (right) expressing Sty1p-GFP. Sty1p-GFP accumulated in the nuclei of many *pkd2* mutants (arrow heads). Maxim intensity projections of Z-series are shown. (C) Time lapse micrographs of a *pkd2-81KD* cell expressing Sty1p-GFP when it deflated. Both bright field (top) and fluorescence images (bottom) of the cell are shown. Number represents time in minutes. (D) Average time course of relative sizes (red circles and red line) and fluorescence intensities of nuclear Sty1p-GFP (Blue squares and blue line) of *pkd2-81KD* cells (n = 7) during their deflation and recovery. Error bars are standard deviation. Time zero is defined as the start of deflation. Bars represent 5 μm.

Figure 8. Stress interrupted both mitosis and cytokinesis in *pkd2-81KD* cells. (A) Time lapse fluorescence micrographs of a wild type (*pkd2*$^{+}$, top) and a *pkd2-81KD* cell (middle) expressing Atb2p-mCherry in mitosis. Bottom: the bright field micrographs of the *pkd2* mutant cell. Mitosis

paused in the *pkd2-81KD* cell when it deflated (red underline). Numbers represent times in min. (B) Time lapse fluorescence micrographs of cytokinesis in two *pkd2-81KD* cells expressing Rlc1p-tdTomato. The contractile rings were compressed (red underline) during either the maturation (top) or the constriction (bottom). Only the cell division sites are shown. The interval between each frame is 2 min. Bars are 5 μm.

Figure 9. A model for the function of Pkd2p in cytokinesis. Cartoon representation of a model of recruitment and activation of Pkd2p as a mechanosensitive channel at the cleavage furrow in fission yeast cytokinesis. The contractile ring (blue) recruits inactive Pkd2p channel (yellow) to the cleavage furrow. When the contractile ring starts to constrict, Pkd2p is activated by the mechanical force (red arrows) that is applied by both the ring and the septum. Activated Pkd2p channels (red) attenuate the contractile ring constriction and the SIN pathway in cytokinesis, potentially through regulating the intracellular concentration of Ca^{2+}.

Figure S1. Pkd2p-GFP is an essential fission yeast TRP protein localized to the cleavage furrow, related to Fig. 1 and 2. . (A) Fluorescence micrographs of fission yeast cells expressing Pkd2p-GFP (green) and Rlc1p-tdTomato (red) treated with LatA, an actin filament depolymerizing drug. Pkd2p-GFP was displaced from its localization at the cleavage furrow in cytokinesis after being treated with 10 μM LatA for 30 mins. It localized to punta in the cortex adjacent to the clumps labeled by Rlc1p-tdTomato. (B) Fluorescence micrographs of fission yeast cells expressing Pkd2p-GFP treated with MBC, a microtubule depolymerizing drug. Pkd2p-GFP maintains its localization at the cleavage furrow (red arrow heads) in cytokinesis after being treated with 50 μM MBC for 30 mins.

Figure S2. The *pkd2* mutant, *pkd2-81KD*, has defect in both cytokinesis and septation. (A) Fluorescence micrographs of the wild type cells expressing Sty1p-mEGFP in either YE5s (left)

or YE5s plus 1M KCl (right). (B) Left: a fluorescence micrograph of three linked *pkd2-81KD* cells expressing GFP-Lifeact. Right: a fluorescence kymograph of the three cells, based on a 60s time-lapse video with 1s interval. Turnover of actin patches stopped temporarily in the deflated *pkd2-81KD* cell (top). Among the three cells, actin patches underwent quick turnover, shown as numerous short tracks in the kymograph, in the two inflated cells while those in the deflated cell did not.

Supplemental materials:

Movie S1: A fluorescence time-lapse video of *pkd2-81KD* cells expressing Pkd2p-mEGFP (green) and Rlc1p-tdTomato (red). Maxim intensity projections of Z-series are shown.

Movie S2: A bright field time-lapse video of *pkd2-81KD* cells in the abscission stage of cytokinesis.

Movie S3: A fluorescence time-lapse video of the wild type cells expressing Sad1-mGFP (green) and Rlc1p-tdTomato (red). Maxim intensity projections of Z-series are shown.

Movie S4: A fluorescence time-lapse video of a *pkd2-81KD* cell expressing Sad1-mGFP (green) and Rlc1p-tdTomato (red). Maxim intensity projections of Z-series are shown.

Movie S5: A bright-field time-lapse video of *pkd2-81KD* cells oscillating between "deflated" and "inflated" states.

Movie S6: A fluorescence time-lapse video of *pkd2-81KD* cells expressing Sty1p-mEGFP, acquired with fluorescence microscopy. Maxim intensity projections of Z-series are shown.

Movie S7: A time-lapse video of a *pkd2-81KD* mutant cells expressing Rlc1p-tdTomato when it deflated, acquired with fluorescence microscopy. Maxim intensity projections of Z-series are shown.

Movie S8: A time-lapse video of a *pkd2-81KD* mutant cells expressing mCherry-Atb2p during its deflation, acquired with fluorescence microscopy. Maxim intensity projections of Z-series are shown.

Table S1: Yeast strains used in this study.

Table S1: Yeast strains used in this study

Name	Genotype	Source
QC-Y690	*h- pkd2-mEGFP-kanMX6*	This study
QC-Y679	*h- trp663-mEGFP-KanMX6*	This study
QC-Y680	*h- trp1322-mEGFP-kanMX6*	This study
QC-Y693	*h? pkd2-mGFP-kanMX6 rlc1-tdTomato-NatMX6*	This study
QC-Y712	*h-/h+ pkd2::kanMX6/pkd2*$^{+}$	This study
QC-Y802	*h- kanMX6-P3nmt1-pkd2*	This study
QC-Y740	*h- kanMX6-41nmt1-pkd2*	This study
QC-Y810	*h- KanMX6-P81nmt1-pkd2*	This study
QC-Y817	*h+ KanMX6-P81nmt1-pkd2*	This study
QC-Y274	*h- rlc1-tdTomato-NatMX6 sad1-GFP-KanMX6*	Lab stock
JW1341	*h- rlc1-tdTomato-NatMX6*	Lab stock
QC-Y813	*h? kanMX6-81xnmt1-Pkd2 rlc1-tdTomato-NatMX6*	Lab stock
QC-Y814	*h? kanMX6-81xnmt1-Pkd2 rlc1-tdTomato-NatMX6 sad1-mEGFP-KanMX6*	This study
QC-Y277	*h- leu1-32 ura4-D18 his-D1 bgs1::ura4+ Pbgs1:: GFP-bgs1:leu1*	Juan Carlos
QC-Y816	*kanMX6-81xnmt1-Pkd2 bgs1::ura4+ Pbgs1:: GFP-bgs1:leu1*	This study
QC-Y276	*h+ leu1-32 ura4-18 his3-1 bgs4::ura4+ Pbgs4+::GFP-bgs4+:leu1+*	Juan Carlos
QC-Y828	*h? kanMX6-81xnmt1-pkd2 bgs4::ura4+ Pbgs4+::GFP-bgs4+:leu1+*	This study
YDM3044	*h- mob1-R4*	Lab stock
QC-Y826	*h? kanMX6-81xnmt1-Pkd2 mob1-R4*	This study
YDM429	*h+ sid2-250*	Lab stock
QC-Y825	*h? kanMX6-81xnmt1-Pkd2 sid2-250*	This study
QC-Y871	*h- sty1-mEGFP-KanMX6*	This study
QC-Y877	*h? sty1-mEGFP-KanMX6 kanMX6-81xnmt1-Pkd2*	This study
QC-Y841	*h? kanMX6-81xnmt1-Pkd2 Kan-Padf1-mEGFP-Lifeact*	This study
DM4762	*h- leu1-32 ura4-Δ18 mCherry-ATB2::HphR*	Lab stock
QC-Y857	*h? kanMX6-81xnmt1-Pkd2 mcherry-atb2::HghR*	This study

References:

Aydar, E., and C.P. Palmer. 2009. Polycystic kidney disease channel and synaptotagmin homologues play roles in schizosaccharomyces pombe cell wall synthesis/repair and membrane protein trafficking. *The Journal of membrane biology*. 229:141-152.

Bahler, J., J.Q. Wu, M.S. Longtine, N.G. Shah, A. McKenzie, 3rd, A.B. Steever, A. Wach, P. Philippsen, and J.R. Pringle. 1998. Heterologous modules for efficient and versatile PCR-based gene targeting in Schizosaccharomyces pombe. *Yeast (Chichester, England)*. 14:943-951.

Balasubramanian, M.K., D. McCollum, L. Chang, K.C. Wong, N.I. Naqvi, X. He, S. Sazer, and K.L. Gould. 1998. Isolation and characterization of new fission yeast cytokinesis mutants. *Genetics*. 149:1265-1275.

Barr, M.M., J. DeModena, D. Braun, C.Q. Nguyen, D.H. Hall, and P.W. Sternberg. 2001. The Caenorhabditis elegans autosomal dominant polycystic kidney disease gene homologs lov-1 and pkd-2 act in the same pathway. *Curr Biol*. 11:1341-1346.

Barr, M.M., and P.W. Sternberg. 1999. A polycystic kidney-disease gene homologue required for male mating behaviour in C. elegans. *Nature*. 401:386-389.

Basi, G., E. Schmid, and K. Maundrell. 1993. TATA box mutations in the Schizosaccharomyces pombe nmt1 promoter affect transcription efficiency but not the transcription start point or thiamine repressibility. *Gene*. 123:131-136.

Chan, C.M., J.T. Aw, S.E. Webb, and A.L. Miller. 2016. SOCE proteins, STIM1 and Orai1, are localized to the cleavage furrow during cytokinesis of the first and second cell division cycles in zebrafish embryos. *Zygote*. 24:880-889.

Chan, C.M., Y. Chen, T.S. Hung, A.L. Miller, A.M. Shipley, and S.E. Webb. 2015. Inhibition of SOCE disrupts cytokinesis in zebrafish embryos via inhibition of cleavage furrow deepening. *The International journal of developmental biology*. 59:289-301.

Chang, F., D. Drubin, and P. Nurse. 1997. cdc12p, a protein required for cytokinesis in fission yeast, is a component of the cell division ring and interacts with profilin. *The Journal of cell biology*. 137:169-182.

Chen, Q., and T.D. Pollard. 2011. Actin filament severing by cofilin is more important for assembly than constriction of the cytokinetic contractile ring. *The Journal of cell biology*. 195:485-498.

Chen, Q., and T.D. Pollard. 2013. Actin filament severing by cofilin dismantles actin patches and produces mother filaments for new patches. *Curr Biol*. 23:1154-1162.

Cortes, J.C., M. Sato, J. Munoz, M.B. Moreno, J.A. Clemente-Ramos, M. Ramos, H. Okada, M. Osumi, A. Duran, and J.C. Ribas. 2012. Fission yeast Ags1 confers the essential septum strength needed for safe gradual cell abscission. *The Journal of cell biology*. 198:637-656.

Courtemanche, N., T.D. Pollard, and Q. Chen. 2016. Avoiding artefacts when counting polymerized actin in live cells with LifeAct fused to fluorescent proteins. *Nature cell biology*. 18:676-683.

De Lozanne, A., and J.A. Spudich. 1987. Disruption of the Dictyostelium myosin heavy chain gene by homologous recombination. *Science (New York, N.Y)*. 236:1086-1091.

Degols, G., K. Shiozaki, and P. Russell. 1996. Activation and regulation of the Spc1 stress-activated protein kinase in Schizosaccharomyces pombe. *Mol Cell Biol*. 16:2870-2877.

Effler, J.C., Y.S. Kee, J.M. Berk, M.N. Tran, P.A. Iglesias, and D.N. Robinson. 2006. Mitosis-specific mechanosensing and contractile-protein redistribution control cell shape. *Curr Biol*. 16:1962-1967.

Fluck, R.A., A.L. Miller, and L.F. Jaffe. 1991. Slow calcium waves accompany cytokinesis in medaka fish eggs. *The Journal of cell biology*. 115:1259-1265.

Gaits, F., G. Degols, K. Shiozaki, and P. Russell. 1998. Phosphorylation and association with the transcription factor Atf1 regulate localization of Spc1/Sty1 stress-activated kinase in fission yeast. *Genes & development*. 12:1464-1473.

Gao, Z., D.M. Ruden, and X. Lu. 2003. PKD2 cation channel is required for directional sperm movement and male fertility. *Curr Biol*. 13:2175-2178.

Gonzalez-Perrett, S., M. Batelli, K. Kim, M. Essafi, G. Timpanaro, N. Moltabetti, I.L. Reisin, M.A. Arnaout, and H.F. Cantiello. 2002. Voltage dependence and pH regulation of human polycystin-2-mediated cation channel activity. *The Journal of biological chemistry*. 277:24959-24966.

Gonzalez-Perrett, S., K. Kim, C. Ibarra, A.E. Damiano, E. Zotta, M. Batelli, P.C. Harris, I.L. Reisin, M.A. Arnaout, and H.F. Cantiello. 2001. Polycystin-2, the protein mutated in autosomal dominant polycystic kidney disease (ADPKD), is a Ca2+-permeable nonselective cation channel. *Proceedings of the National Academy of Sciences of the United States of America*. 98:1182-1187.

Grieben, M., A.C. Pike, C.A. Shintre, E. Venturi, S. El-Ajouz, A. Tessitore, L. Shrestha, S. Mukhopadhyay, P. Mahajan, R. Chalk, N.A. Burgess-Brown, R. Sitsapesan, J.T. Huiskonen, and E.P. Carpenter. 2017. Structure of the polycystic kidney disease TRP channel Polycystin-2 (PC2). *Nat Struct Mol Biol*. 24:114-122.

Hou, M.C., J. Salek, and D. McCollum. 2000. Mob1p interacts with the Sid2p kinase and is required for cytokinesis in fission yeast. *Curr Biol*. 10:619-622.

Hughes, J., C.J. Ward, B. Peral, R. Aspinwall, K. Clark, J.L. San Millan, V. Gamble, and P.C. Harris. 1995. The polycystic kidney disease 1 (PKD1) gene encodes a novel protein with multiple cell recognition domains. *Nature genetics*. 10:151-160.

Inohara, N., and G. Nunez. 2002. ML -- a conserved domain involved in innate immunity and lipid metabolism. *Trends in biochemical sciences*. 27:219-221.

Johnson, A.E., D. McCollum, and K.L. Gould. 2012. Polar opposites: Fine-tuning cytokinesis through SIN asymmetry. *Cytoskeleton (Hoboken)*. 69:686-699.

Kung, C. 2005. A possible unifying principle for mechanosensation. *Nature*. 436:647-654.

Laplante, C., J. Berro, E. Karatekin, A. Hernandez-Leyva, R. Lee, and T.D. Pollard. 2015. Three myosins contribute uniquely to the assembly and constriction of the fission yeast cytokinetic contractile ring. *Curr Biol*. 25:1955-1965.

Liu, J., H. Wang, D. McCollum, and M.K. Balasubramanian. 1999. Drc1p/Cps1p, a 1,3-beta-glucan synthase subunit, is essential for division septum assembly in Schizosaccharomyces pombe. *Genetics*. 153:1193-1203.

Liu, X., T. Vien, J. Duan, S.H. Sheu, P.G. DeCaen, and D.E. Clapham. 2018. Polycystin-2 is an essential ion channel subunit in the primary cilium of the renal collecting duct epithelium. *eLife*. 7.

Ma, Y., R. Sugiura, A. Koike, H. Ebina, S.O. Sio, and T. Kuno. 2011. Transient receptor potential (TRP) and Cch1-Yam8 channels play key roles in the regulation of cytoplasmic Ca2+ in fission yeast. *PLoS One*. 6:e22421.

Martinac, B., M. Buechner, A.H. Delcour, J. Adler, and C. Kung. 1987. Pressure-sensitive ion channel in Escherichia coli. *Proceedings of the National Academy of Sciences of the United States of America*. 84:2297-2301.

Maundrell, K. 1990. nmt1 of fission yeast. A highly transcribed gene completely repressed by thiamine. *The Journal of biological chemistry*. 265:10857-10864.

McDonald, N.A., A.L. Lind, S.E. Smith, R. Li, and K.L. Gould. 2017. Nanoscale architecture of the Schizosaccharomyces pombe contractile ring. *eLife*. 6.

Millar, J.B., V. Buck, and M.G. Wilkinson. 1995. Pyp1 and Pyp2 PTPases dephosphorylate an osmosensing MAP kinase controlling cell size at division in fission yeast. *Genes & development*. 9:2117-2130.

Miller, A.L., R.A. Fluck, J.A. McLaughlin, and L.F. Jaffe. 1993. Calcium buffer injections inhibit cytokinesis in Xenopus eggs. *Journal of cell science*. 106 (Pt 2):523-534.

Mishra, M., J. Kashiwazaki, T. Takagi, R. Srinivasan, Y. Huang, M.K. Balasubramanian, and I. Mabuchi. 2013. In vitro contraction of cytokinetic ring depends on myosin II but not on actin dynamics. *Nature cell biology*. 15:853-859.

Mochizuki, T., G. Wu, T. Hayashi, S.L. Xenophontos, B. Veldhuisen, J.J. Saris, D.M. Reynolds, Y. Cai, P.A. Gabow, A. Pierides, W.J. Kimberling, M.H. Breuning, C.C. Deltas, D.J. Peters, and S. Somlo. 1996. PKD2, a gene for polycystic kidney disease that encodes an integral membrane protein. *Science (New York, N.Y)*. 272:1339-1342.

Montell, C., and G.M. Rubin. 1989. Molecular characterization of the Drosophila trp locus: a putative integral membrane protein required for phototransduction. *Neuron*. 2:1313-1323.

Munoz, J., J.C. Cortes, M. Sipiczki, M. Ramos, J.A. Clemente-Ramos, M.B. Moreno, I.M. Martins, P. Perez, and J.C. Ribas. 2013. Extracellular cell wall beta(1,3)glucan is required to couple septation to actomyosin ring contraction. *The Journal of cell biology*. 203:265-282.

Nauli, S.M., F.J. Alenghat, Y. Luo, E. Williams, P. Vassilev, X. Li, A.E. Elia, W. Lu, E.M. Brown, S.J. Quinn, D.E. Ingber, and J. Zhou. 2003. Polycystins 1 and 2 mediate mechanosensation in the primary cilium of kidney cells. *Nature genetics*. 33:129-137.

Noguchi, T., and I. Mabuchi. 2002. Localized calcium signals along the cleavage furrow of the Xenopus egg are not involved in cytokinesis. *Molecular biology of the cell*. 13:1263-1273.

Palmer, C.P., E. Aydar, and M.B. Djamgoz. 2005. A microbial TRP-like polycystic-kidney-disease-related ion channel gene. *The Biochemical journal*. 387:211-219.

Palmer, C.P., X.L. Zhou, J. Lin, S.H. Loukin, C. Kung, and Y. Saimi. 2001. A TRP homolog in Saccharomyces cerevisiae forms an intracellular Ca(2+)-permeable channel in the yeast vacuolar membrane. *Proceedings of the National Academy of Sciences of the United States of America*. 98:7801-7805.

Pennekamp, P., C. Karcher, A. Fischer, A. Schweickert, B. Skryabin, J. Horst, M. Blum, and B. Dworniczak. 2002. The ion channel polycystin-2 is required for left-right axis determination in mice. *Curr Biol*. 12:938-943.

Pollard, T.D. 2010. Mechanics of cytokinesis in eukaryotes. *Current opinion in cell biology*. 22:50-56.

Pollard, T.D., and J.Q. Wu. 2010. Understanding cytokinesis: lessons from fission yeast. *Nature reviews*. 11:149-155.

Proctor, S.A., N. Minc, A. Boudaoud, and F. Chang. 2012. Contributions of turgor pressure, the contractile ring, and septum assembly to forces in cytokinesis in fission yeast. *Curr Biol*. 22:1601-1608.

Protchenko, O., R. Rodriguez-Suarez, R. Androphy, H. Bussey, and C.C. Philpott. 2006. A screen for genes of heme uptake identifies the FLC family required for import of FAD into the endoplasmic reticulum. *The Journal of biological chemistry*. 281:21445-21457.

Qian, F., F.J. Germino, Y. Cai, X. Zhang, S. Somlo, and G.G. Germino. 1997. PKD1 interacts with PKD2 through a probable coiled-coil domain. *Nature genetics*. 16:179-183.

Rappaport, R. 1967. Cell division: direct measurement of maximum tension exerted by furrow of echinoderm eggs. *Science (New York, N.Y)*. 156:1241-1243.

Rigamonti, M., S. Groppi, F. Belotti, R. Ambrosini, G. Filippi, E. Martegani, and R. Tisi. 2015. Hypotonic stress-induced calcium signaling in Saccharomyces cerevisiae involves TRP-like transporters on the endoplasmic reticulum membrane. *Cell calcium*. 57:57-68.

Sanger, J.M., and J.W. Sanger. 1980. Banding and polarity of actin filaments in interphase and cleaving cells. *The Journal of cell biology*. 86:568-575.

Shen, P.S., X. Yang, P.G. DeCaen, X. Liu, D. Bulkley, D.E. Clapham, and E. Cao. 2016. The Structure of the Polycystic Kidney Disease Channel PKD2 in Lipid Nanodiscs. *Cell*. 167:763-773 e711.

Shiozaki, K., and P. Russell. 1995. Cell-cycle control linked to extracellular environment by MAP kinase pathway in fission yeast. *Nature*. 378:739-743.

Simanis, V. 2015. Pombe's thirteen - control of fission yeast cell division by the septation initiation network. *Journal of cell science*. 128:1465-1474.

Sirotkin, V., J. Berro, K. Macmillan, L. Zhao, and T.D. Pollard. 2010. Quantitative analysis of the mechanism of endocytic actin patch assembly and disassembly in fission yeast. *Molecular biology of the cell*. 21:2894-2904.

Sparks, C.A., M. Morphew, and D. McCollum. 1999. Sid2p, a spindle pole body kinase that regulates the onset of cytokinesis. *The Journal of cell biology*. 146:777-790.

Srivastava, V., P.A. Iglesias, and D.N. Robinson. 2016. Cytokinesis: Robust cell shape regulation. *Seminars in cell & developmental biology*. 53:39-44.

Stachowiak, M.R., C. Laplante, H.F. Chin, B. Guirao, E. Karatekin, T.D. Pollard, and B. O'Shaughnessy. 2014. Mechanism of cytokinetic contractile ring constriction in fission yeast. *Developmental cell*. 29:547-561.

Straight, A.F., A. Cheung, J. Limouze, I. Chen, N.J. Westwood, J.R. Sellers, and T.J. Mitchison. 2003. Dissecting temporal and spatial control of cytokinesis with a myosin II Inhibitor. *Science (New York, N.Y)*. 299:1743-1747.

Thevenaz, P., U.E. Ruttimann, and M. Unser. 1998. A pyramid approach to subpixel registration based on intensity. *IEEE transactions on image processing : a publication of the IEEE Signal Processing Society*. 7:27-41.

Tsiokas, L., E. Kim, T. Arnould, V.P. Sukhatme, and G. Walz. 1997. Homo- and heterodimeric interactions between the gene products of PKD1 and PKD2. *Proceedings of the National Academy of Sciences of the United States of America*. 94:6965-6970.

Vazquez, H.M., C. Vionnet, C. Roubaty, S.K. Mallela, R. Schneiter, and A. Conzelmann. 2016. Chemogenetic E-MAP in Saccharomyces cerevisiae for Identification of Membrane Transporters Operating Lipid Flip Flop. *PLoS genetics*. 12:e1006160.

Walker, R.G., A.T. Willingham, and C.S. Zuker. 2000. A Drosophila mechanosensory transduction channel. *Science (New York, N.Y)*. 287:2229-2234.

Watnick, T.J., Y. Jin, E. Matunis, M.J. Kernan, and C. Montell. 2003. A flagellar polycystin-2 homolog required for male fertility in Drosophila. *Curr Biol*. 13:2179-2184.

Wilkes, M., M.G. Madej, L. Kreuter, D. Rhinow, V. Heinz, S. De Sanctis, S. Ruppel, R.M. Richter, F. Joos, M. Grieben, A.C. Pike, J.T. Huiskonen, E.P. Carpenter, W. Kuhlbrandt, R. Witzgall, and C. Ziegler. 2017. Molecular insights into lipid-assisted Ca2+ regulation of the TRP channel Polycystin-2. *Nat Struct Mol Biol*. 24:123-130.

Wu, G., V. D'Agati, Y. Cai, G. Markowitz, J.H. Park, D.M. Reynolds, Y. Maeda, T.C. Le, H. Hou, Jr., R. Kucherlapati, W. Edelmann, and S. Somlo. 1998. Somatic inactivation of Pkd2 results in polycystic kidney disease. *Cell*. 93:177-188.

Wu, G., G.S. Markowitz, L. Li, V.D. D'Agati, S.M. Factor, L. Geng, S. Tibara, J. Tuchman, Y. Cai, J.H. Park, J. van Adelsberg, H. Hou, Jr., R. Kucherlapati, W. Edelmann, and S. Somlo. 2000. Cardiac defects and renal failure in mice with targeted mutations in Pkd2. *Nature genetics*. 24:75-78.

Wu, J.Q., J.R. Kuhn, D.R. Kovar, and T.D. Pollard. 2003. Spatial and temporal pathway for assembly and constriction of the contractile ring in fission yeast cytokinesis. *Developmental cell*. 5:723-734.

Wu, J.Q., and T.D. Pollard. 2005. Counting cytokinesis proteins globally and locally in fission yeast. *Science (New York, N.Y)*. 310:310-314.

Wu, L.J., T.B. Sweet, and D.E. Clapham. 2010. International Union of Basic and Clinical Pharmacology. LXXVI. Current progress in the mammalian TRP ion channel family. *Pharmacological reviews*. 62:381-404.

Figure 1

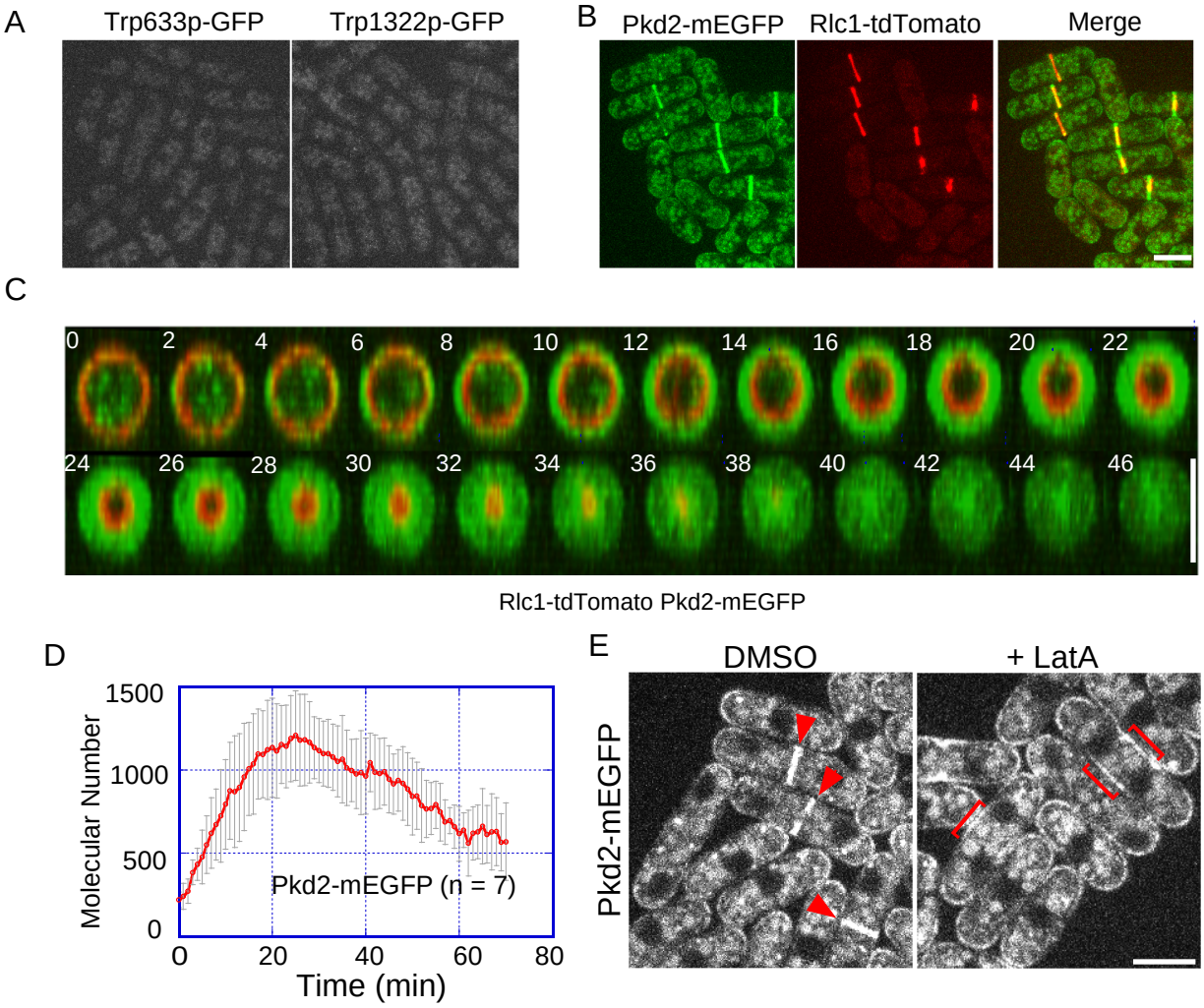

Figure 2

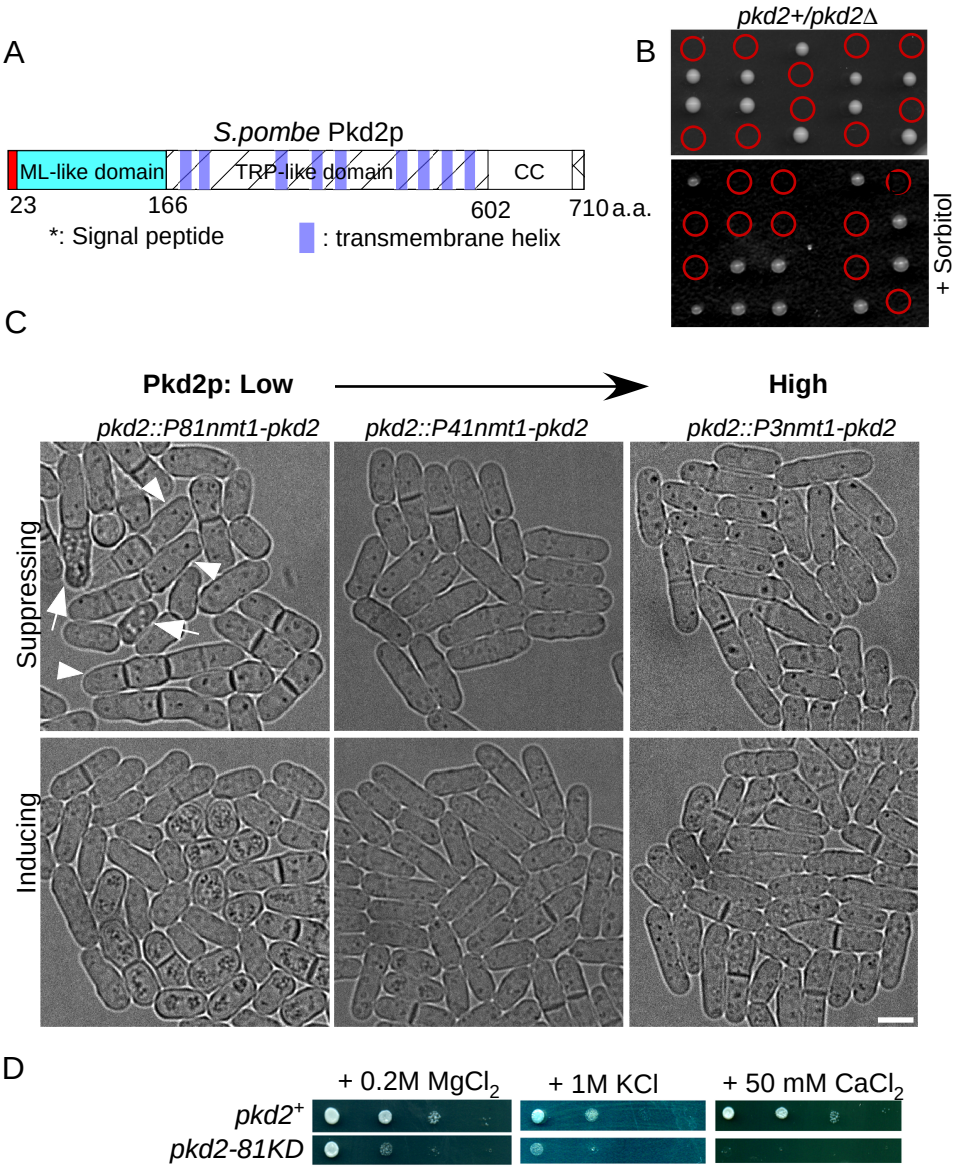

Figure 3

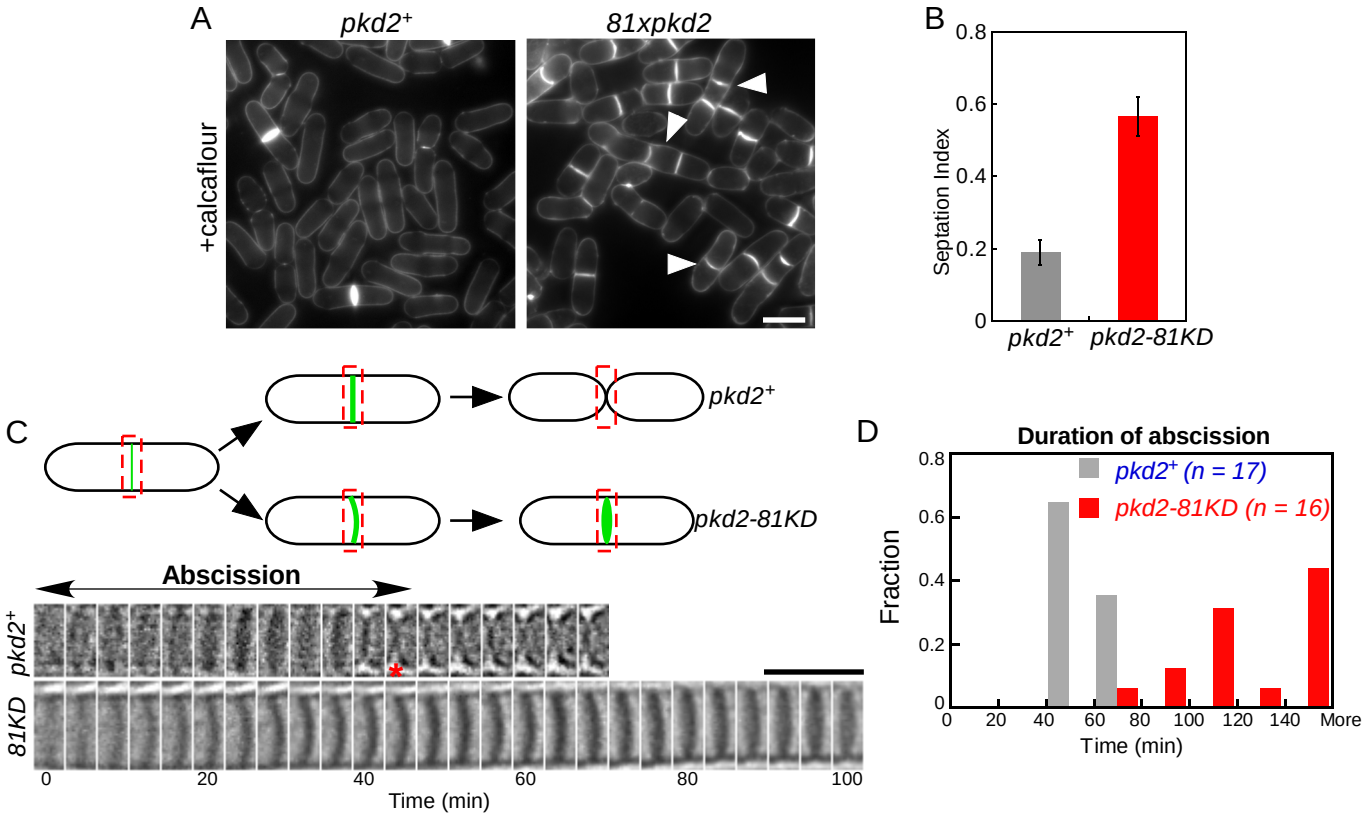

Figure 4

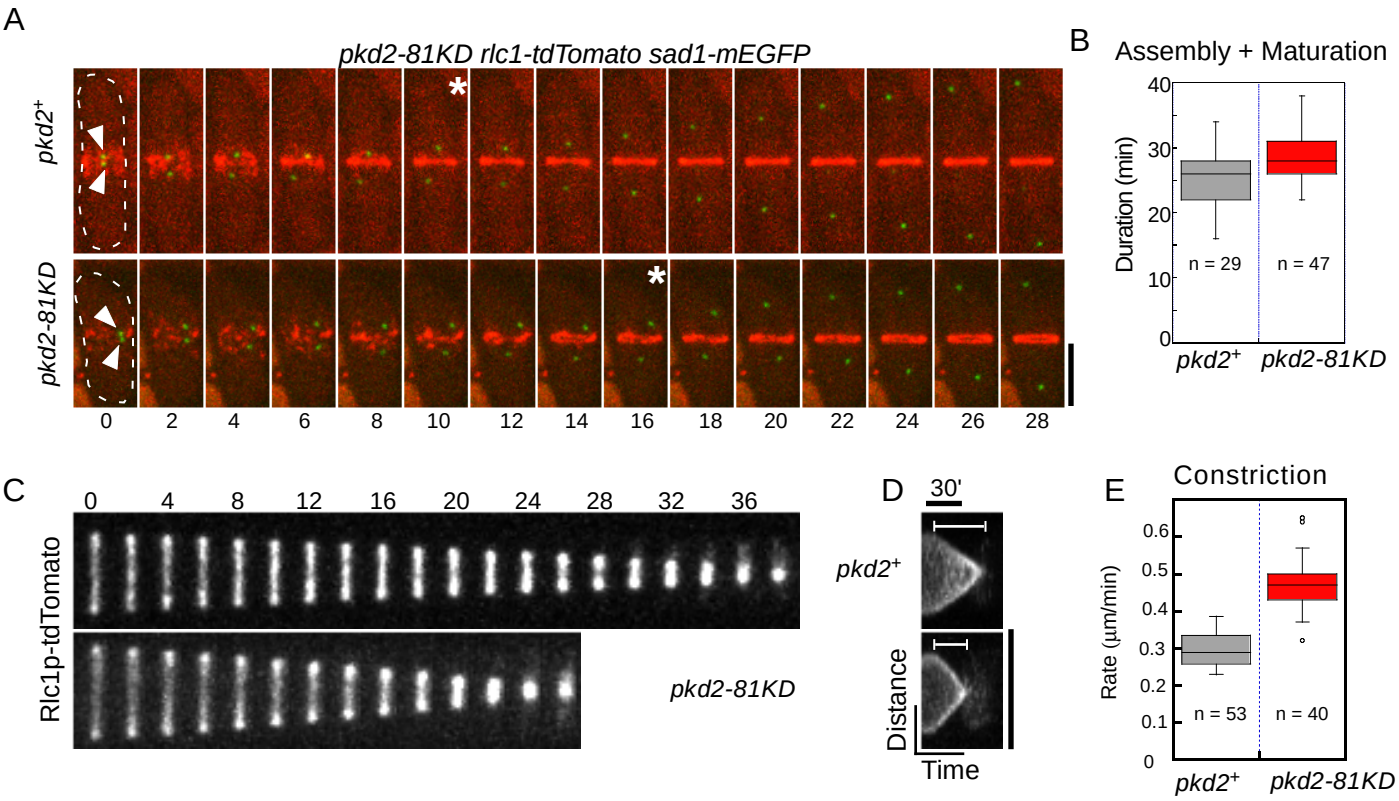

Figure 5

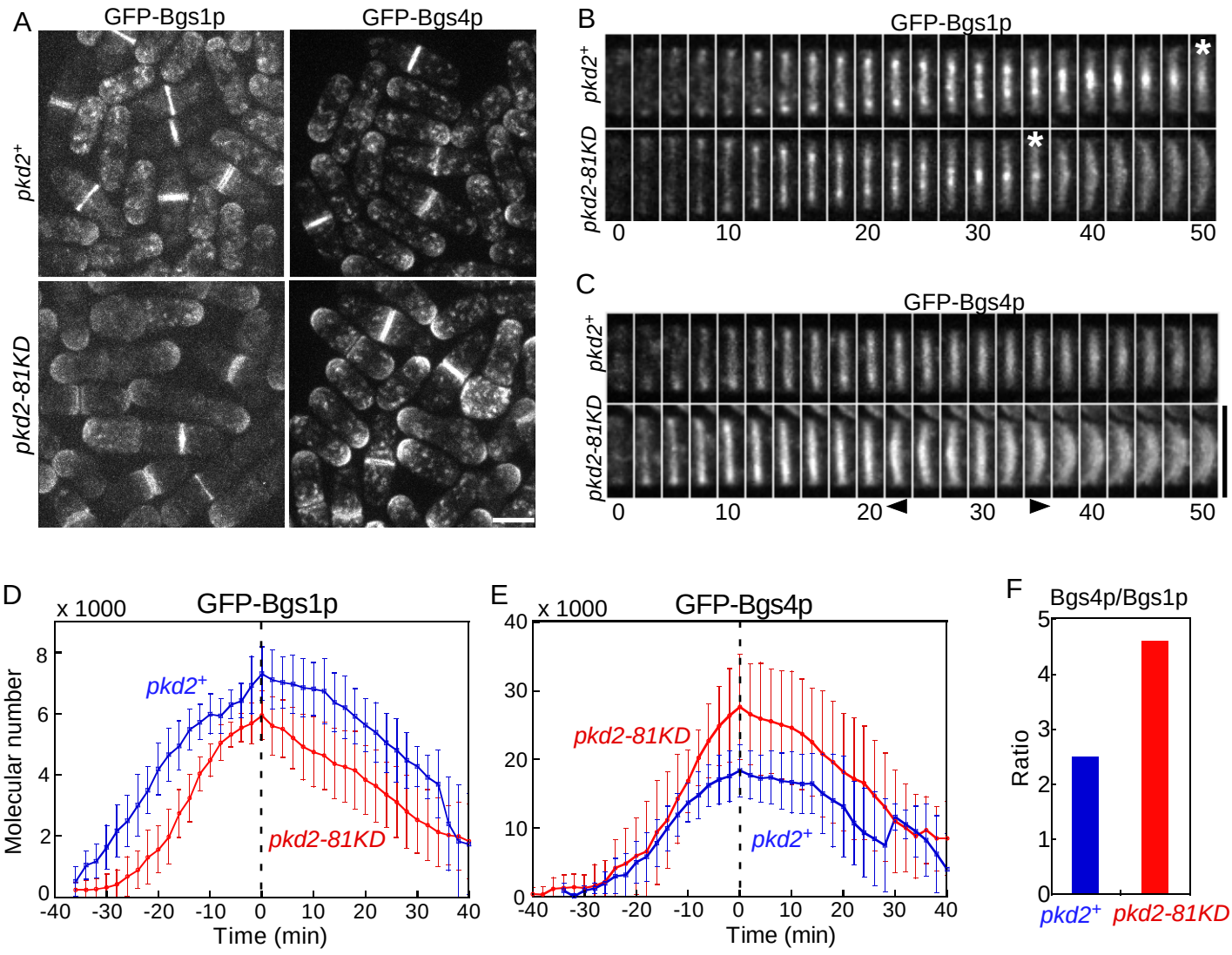

Figure 6

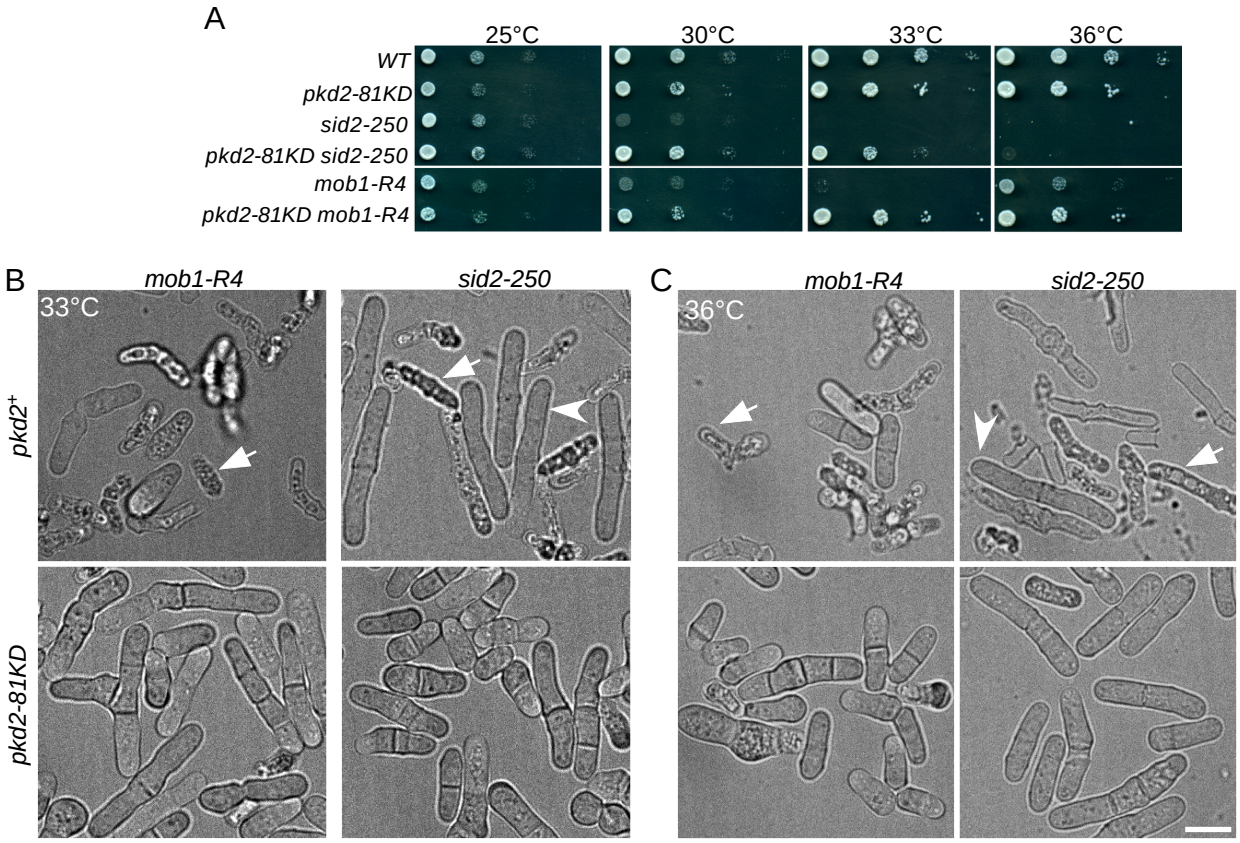

Figure 7

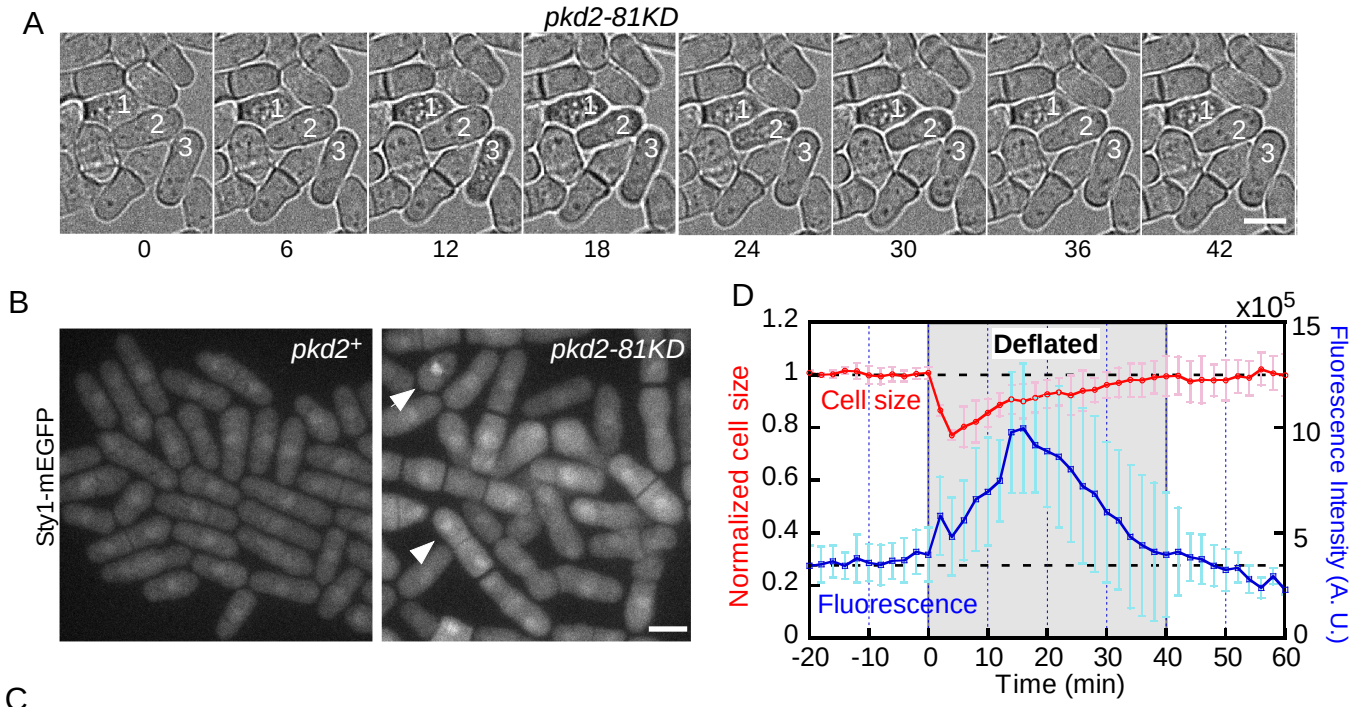

Figure 8

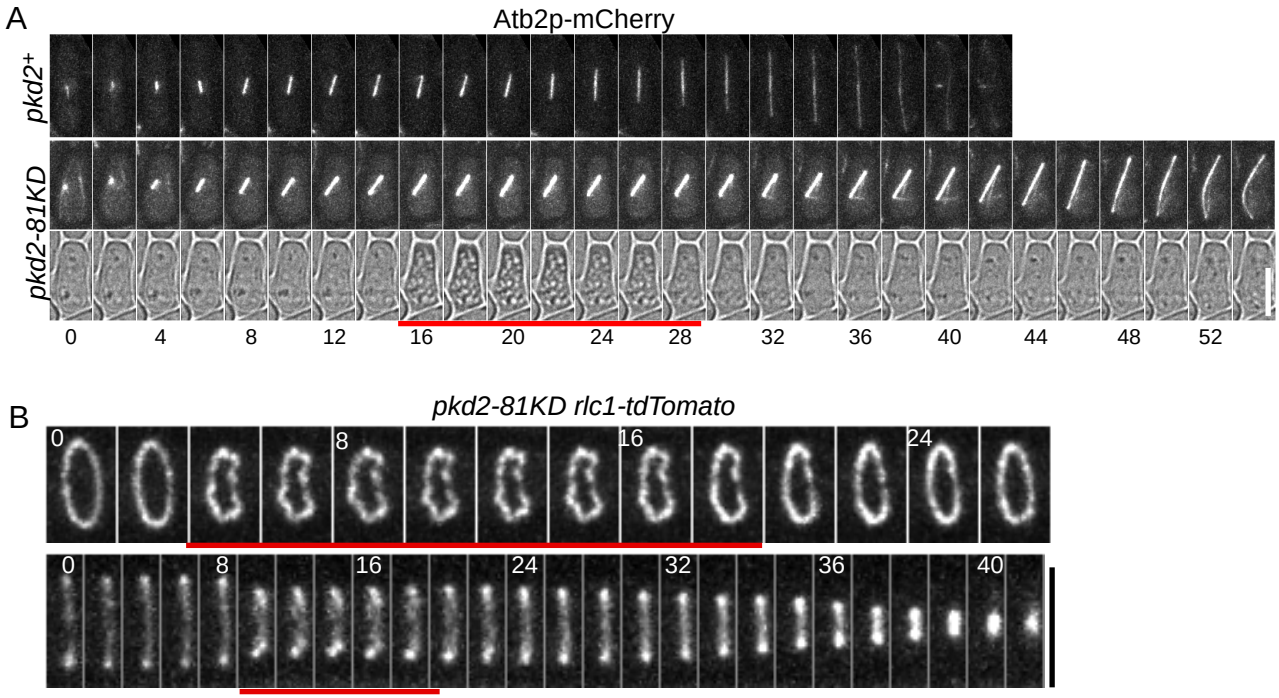

Figure 9

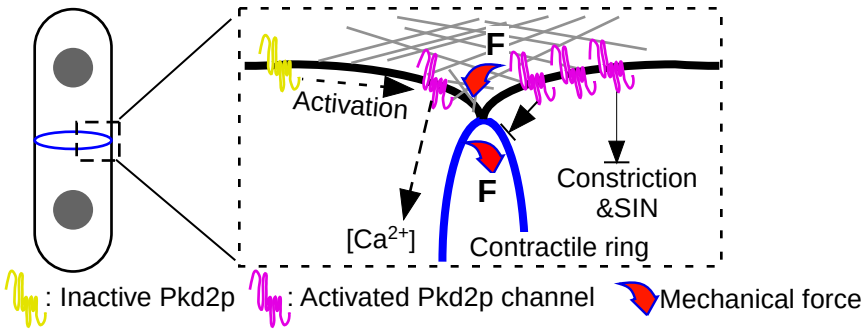

Figure S1

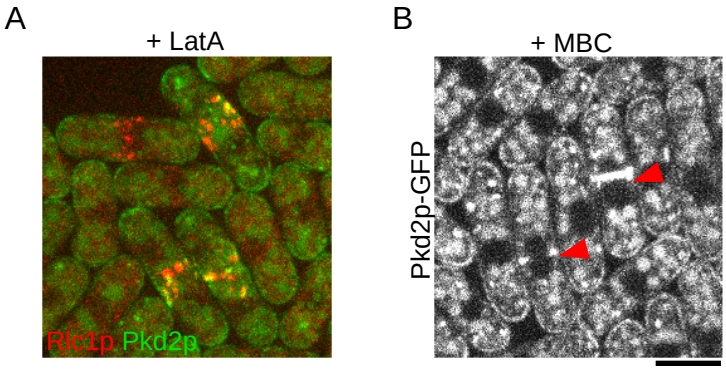

Figure S2